

Ab initio calculation of elastic properties of solid He under pressureZ. Nabi,¹ L. Vitos,^{1,2,3} B. Johansson,^{1,2,4} and R. Ahuja^{1,2}¹Condensed Matter Theory Group, Department of Physics, Uppsala University, Box 530, S-751 21, Uppsala, Sweden²Applied Materials Physics, Department of Materials Science and Engineering, Royal Institute of Technology, SE-100 44 Stockholm, Sweden³Research Institute for Solid State Physics and Optics, P.O. Box 49, H-1525 Budapest, Hungary⁴AB Sandvik Materials Technology, SE-811 81 Sandviken, Sweden

(Received 9 July 2005; published 7 November 2005)

The high-pressure equation of state and elastic properties of solid He (⁴He) have been calculated using density functional theory formulated in the framework of the exact muffin-tin orbitals method. The theoretical results, obtained within the generalized gradient approximation for the exchange-correlation functional, are in good agreement with the experimental data available for pressures between 13 GPa and 32 GPa. We predict that at 0 K the hexagonal phase of He remains mechanically and thermodynamically stable up to the highest pressure considered in the present study (~ 150 GPa). The calculated anisotropy ratios of He are similar to those observed in the case of hexagonal metals with $c/a \sim 1.63$. On the other hand, we find that hydrostatic pressure has negligible effect on the anisotropy of He. This indicates that He can be used as a quasihydrostatic medium in high-pressure experiments up to at least 150 GPa.

DOI: [10.1103/PhysRevB.72.172102](https://doi.org/10.1103/PhysRevB.72.172102)

PACS number(s): 62.20.Dc, 64.30.+t, 71.15.Nc, 71.20.Ps

With the refinement of new high-pressure techniques, there has been accelerated interest in the properties of rare gas solids (RGS). Solid helium is one of the most important among the RGS's, because it is considered as the best quasihydrostatic medium.¹⁻⁴ Consequently, modern He-based technologies have made considerable progress in the experimental high-pressure studies. Especially, the diamond anvil cell technique, in conjunction with Brillouin scattering spectroscopy and synchrotron x-ray method, has proved to be a very useful approach for measuring the elasticity of solids at extreme conditions.⁵⁻⁸

An obvious question that is raised in connection with the high-pressure measurements is the hydrostatic limit of the pressure medium.¹ Below this pressure limit, the medium acts as a quasihydrostatic pressure-transmitting environment. At higher pressures nonhydrostaticity develops, which might affect the measured physical properties. During the last few decades, numerous experimental investigations focused on the high-pressure physical properties of solid He.⁹⁻¹⁶ Most recently, Zha *et al.*⁸ determined the complete set of room-temperature single-crystal elastic constant of He between 13 and 32 GPa. From the theoretical side, a number of model calculations were carried out on the dense RGS's.¹⁷⁻²¹ For instance, Tsuchiya and Kawamura,²² using the first-principles theories, calculated the elastic properties of Ne, Ar, Kr, and Xe for pressure up to ~ 100 GPa. However, to our knowledge, no *ab initio* study of the elastic properties of He has been reported so far. The aim of this study is to fill this gap and present a density functional^{23,24} description of the equation of state and elastic properties of solid He under high-pressure.

The self-consistent calculations were performed using the Exact Muffin-Tin Orbitals (EMTO) method.²⁵⁻²⁹ For the exchange-correlation functional we employed the local density approximation (LDA).³⁰ In addition to the LDA, the total energy was calculated using two gradient level approximations, namely the local airy gas (LAG) (Ref. 31) and

generalized gradient (GGA) (Ref. 32) approximations. None of these functionals account for the long-range van der Waals interaction between loosely packed He atoms.³³ Therefore, in the present work we limit our study to high pressures, where the van der Waals term is expected to become minor compared to the many-body interatomic forces.²²

The equation of state of He was determined for the hexagonal close packed (hcp), face centered cubic (fcc), and body centered cubic (bcc) crystallographic structures. The first two structures are present in the low-pressure phase diagram of He,^{14,34,35} whereas the latter was suggested to be the stable phase at very high pressures.^{16,17,19} The total energies were calculated for 12 different volumes between ~ 20 and ~ 60 Bohr³ per atom. According to the experimental equation of state,^{8,34} these volumes correspond, approximately, to pressures between 10 and 150 GPa. For each volume V , the theoretical hexagonal axial ratio $(c/a)_0$ was determined by minimizing the total energy $E(V, c/a)$ of hexagonal structure calculated for 7 c/a ratios close to the energy minimum. For the elastic constant calculation, the bulk modulus B was obtained from a Murnaghan-type function³⁶ fitted to the *ab initio* total energies. Then, the five hexagonal elastic constants c_{11} , c_{12} , c_{13} , c_{33} , and c_{44} were obtained from the bulk modulus, $B = [c_{33}(c_{11} + c_{12}) - 2c_{13}^2]/C$, the logarithmic volume derivative of c/a , $\partial \ln(c/a)_0 / \partial \ln V = -(c_{33} - c_{11} - c_{12} + c_{13})/C$, where $C \equiv c_{11} + c_{12} + 2c_{33} - 4c_{13}$, and three isochoric strains, as described in Ref. 37. Using volume conserving deformations allows us to identify the calculated elastic constants with the stress-strain coefficients used for wave propagation velocity.³⁷⁻³⁹ In the calculations we included the s , p , and d EMTO's. The Green function was calculated for 32 complex energy points distributed exponentially on a semicircular contour enclosing the He $1s^2$ states. For the reciprocal space integrals a sufficiently thick k -mesh was used, so that the total energy for elastic constant calculations was converged to within $\sim 1 \mu\text{Ry}$.

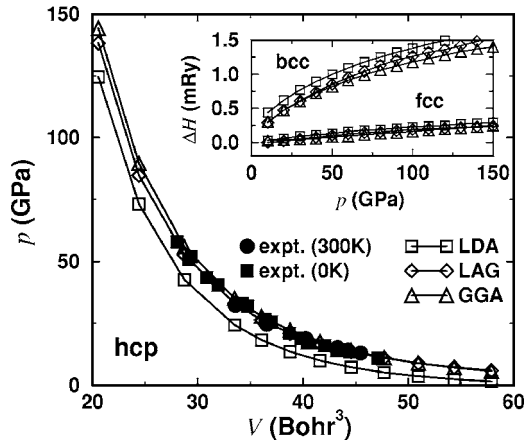


FIG. 1. Theoretical (present results) and experimental equation of state for solid He. The theoretical pressure-volume curves have been obtained using the LDA (open squares), LAG approximation (open diamond), and GGA (open triangle) for the exchange-correlation functional. Filled circles: room-temperature data (Ref. 8); filled squares: temperature reduced data (Ref. 34). In the inset, we show the theoretical enthalpy as a function of pressure for the bcc and fcc structures relative to the stable hcp phase.

At low temperature and pressures below ~ 12 GPa, He crystallizes in the hcp structure.^{14,34,35} With increasing temperature a fcc phase is stabilized from ~ 15 K and ~ 0.1 GPa to ~ 285 K and ~ 12 GPa. Apart from this small fcc stability field, the hcp structure remains the stable phase of solid He up to 58 GPa, the highest pressure considered in experiments.³⁴ The stability of the hcp phase is fully supported by the present theoretical results. In the inset of Fig. 1, we plotted the enthalpy difference ($\Delta H_{\text{fcc}} = H_{\text{fcc}} - H_{\text{hcp}}$) as a function of pressure p . For comparison, in the inset we also show ΔH_{bcc} , obtained for the bcc structure. All three density functionals predict the hcp structure as the most stable low-temperature phase of He. At 10 GPa the calculated LDA, LAG, and GGA enthalpy differences are $\Delta H_{\text{fcc}} = 0.03, 0.01,$ and 0.02 mRy/atom and $\Delta H_{\text{bcc}} = 0.44, 0.28,$ and 0.29 mRy/atom. We find that the pressure further stabilizes the hcp phase relative to the cubic structures, with an average $\partial\Delta H/\partial p$ slope of 0.15 and 0.70 mRy per 100 GPa, for the fcc and bcc structures, respectively.

The LDA, LAG, and GGA equation of states for the hcp He are compared with the available experimental data^{8,34} in Fig. 1. As one can see, the LDA strongly overestimates the bonding, giving $\sim 15\%$ smaller volume near $p = 15$ GPa than the experiment. This overbinding is reduced to below 5% at pressure above 100 GPa. At the same time, both gradient level approximations give results in good agreement with experiments. The correspondence between GGA and experiment is remarkable at pressure $\lesssim 30$ GPa. For higher pressure LAG outperforms the other two approximations.

From a theoretical point of view, it is instructive to investigate the accuracy of the present density functionals at low pressures. With this purpose, we carried out additional self-consistent calculations for volumes between 60 and 300 Bohr³. From these results, for the LDA equilibrium volume we obtain 72 Bohr³. This value is significantly lower

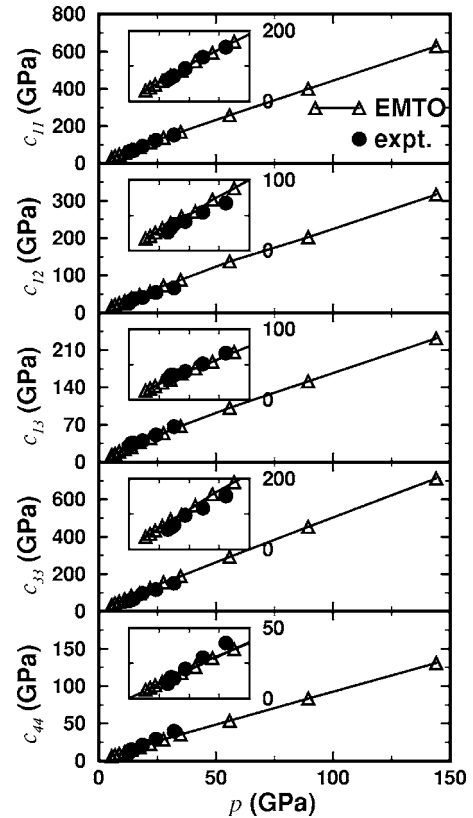


FIG. 2. Elastic constants of hcp He as functions of pressure. Open triangles: present results; filled circles: experimental data (Ref. 8). In the insets, data between 0 and 40 GPa are shown.

than the low-pressure experimental data: 237 Bohr³ at 25 kbar, obtained by Franck and Wenner,⁹ and 309 Bohr³ at zero pressure, quoted by Young.⁴⁰ Within the gradient level approximation, no energy minimum was found in the energy-volume relation, in accordance with Ref. 22. However, because the experimental elastic constant for the hcp He are available for $p = 13\text{--}33$ GPa,⁸ and for this pressure range the GGA was found to give the best agreement with the experimental p - V data, in the rest of the paper we present and discuss only results obtained within this approximation.

The complete set of hexagonal elastic constants is plotted as a function of pressure in Fig. 2. We can see that the theoretical elastic constants agree very well with the available experimental data.⁸ The small discrepancies (see insets) are below the typical errors obtained for the transition metals in conjunction with the GGA.^{31,41,42} We find that all five elastic constants are positive and increase monotonously with p for the entire pressure interval considered in this study. The conditions for the mechanical stability of a hexagonal crystal are: $c_{44} > 0; c_{11} > |c_{12}|, c_{11}c_{33} > (c_{13})^2$ and $c_{33}(c_{11} + c_{12}) > 2(c_{13})^2$.⁴³ The present theoretical c_{ij} values satisfy these conditions for any pressure p , ensuring the mechanical stability of hcp He under pressure.

Within the accuracy of the EMTO method, the axial ratio of the hexagonal He is calculated to be ideal, i.e. $(c/a)_0 \approx 1.63$, and show negligible volume dependence. This is in line with experimental findings below 23.3 GPa.¹⁴ Due to this flat volume dependence of $(c/a)_0$, at each pressure we

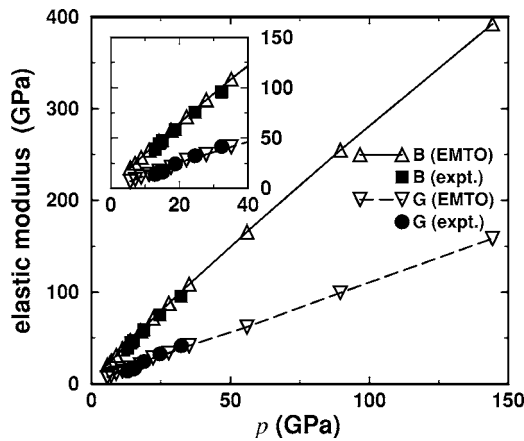


FIG. 3. The bulk and shear modulus of hcp He as a function of pressure. Open triangles: present results; filled circles: experimental data (Ref. 8). In the inset, data between 0 and 40 GPa are shown.

have $c_{33}-c_{11} \approx c_{12}-c_{13}$. The calculated anisotropy of the compressional wave, $\Delta_p = c_{33}/c_{11}$, is 1.12–1.13, and shows no pressure dependence. This result is in slight disagreement with experiment,⁸ where $c_{11} \approx c_{33}$ and $c_{12} \approx c_{13}$ was found within the experimental error bars. Therefore, the theoretical results violates the isotropy condition for a hexagonal symmetry.⁴³ The pressure factors of the two shear wave anisotropies, $\Delta_{S1} \equiv (c_{11}+c_{33}-2c_{13})/4c_{44} = 1.60-1.66$, and $\Delta_{S2} \equiv 2c_{44}/(c_{11}-c_{12}) = 0.87-0.83$, are also calculated to be small. These anisotropy ratios are somewhat different from the experimental ones.⁸ In particular, we find that the calculated Δ_{S1} for He is relatively close to that of solid H₂.⁸ It is interesting to note that the theoretical anisotropy ratios are within the range of those obtained for hexagonal metals with $(c/a)_0 \approx 1.63$. For instance, Mg has $\Delta_p = 1.04$, $\Delta_{S1} = 1.19$, and $\Delta_{S2} = 0.98$. These figures for Co are 1.17, 1.52, 1.06 and for Re are 1.12, 1.36, 0.95.⁴⁴ We conclude that at 0 K the hcp He has similar anisotropy as the hcp metals from the Periodic Table.

In Fig. 3, the theoretical bulk modulus (B) and shear modulus (G) are compared with experimental values.⁸ The polycrystalline shear modulus was calculated from the single-crystal elastic constants using the Voigt-Reuss-Hill averaging method.⁴⁵ The Debye temperature Θ , and the two sound velocities V_p and V_s , derived from the polycrystalline elastic moduli, are plotted in Fig. 4. In both figures, we see a very good agreement between the theoretical and experimental data over the whole pressure range considered in the experiment.

In the Voigt-Reuss-Hill averaging method, one calculates the arithmetic mean of the upper (G_V) and lower (G_R) bounds for the shear modulus. The G_V and G_R bounds can also be used to characterize the polycrystalline solids formed by randomly oriented anisotropic single crystal grains.⁴⁶ These quasi-isotropic materials are isotropic only in a statistical sense, and, therefore, it is useful to define a measure of elastic anisotropy as $A = (G_V - G_R)/(G_V + G_R)$.⁴³ In the case of

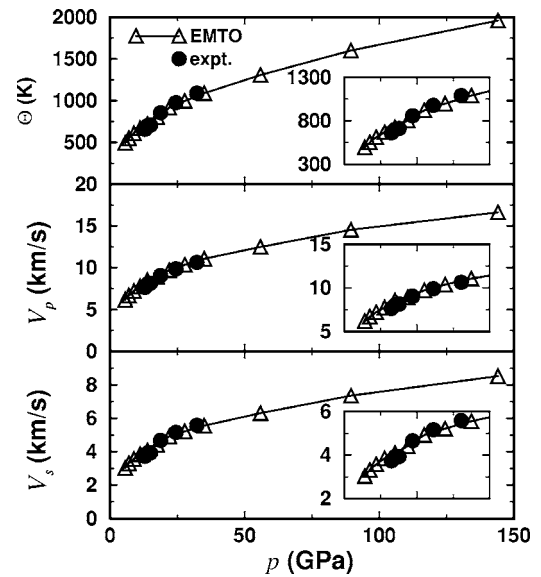


FIG. 4. Debye temperature (upper panel) and sound velocities (middle and lower panels) of hcp He as functions of pressure. Open symbols: present results; filled circles: experimental data (Ref. 8). In the insets, data between 0 and 40 GPa are shown.

hcp He, our calculated anisotropy ratio is ~ 0.02 , and shows negligible pressure dependence. Most of the cubic and low symmetry crystals have elastic anisotropy ratios between 0.0–0.21.^{43,46} On this scale, the anisotropy of hcp He can be considered to be small.

In summary, using the EMTO method, in combination with three density functionals, we have calculated the equation of state and elastic properties of solid He. We have obtained that all three functionals predict the hcp structure as the most stable low-temperature phase of He at pressures between ~ 10 and 150 GPa. At these pressures, the LAG and GGA provide equation of states, which are in excellent agreement with experiments, whereas the LDA strongly overestimates the bonding. The calculated GGA elastic constants are also in good agreement with experimental data. Theory predicts that the anisotropy of hcp He is comparable to that of hexagonal metals with $c/a \approx 1.63$. Therefore, this solid, at least at low temperature, fails to be isotropic. On the other hand, no peculiar features in c_{ij} have been observed with increasing pressures. We have found that the anisotropy ratios of He exhibit a very weak pressure dependence. This result supports that solid He can be used as a quasihydrostatic pressure-transmitting medium in high-pressure devices up to at least 150 GPa.

Work was supported by the Swedish Research Council, the Swedish Foundation for Strategic Research, and the research project OTKA T035043 and T046773 of the Hungarian Scientific Research Fund. SIDA and STINT are also acknowledged for financial support. The calculations were performed at the Swedish National Supercomputer Center.

- ¹K. Takemura, J. Appl. Phys. **89**, 662 (2001).
- ²P. M. Bell and H. K. Mao, Year Book - Carnegie Inst. Washington **80**, 404 (1981).
- ³R. T. Downs, C. S. Zha, T. S. Duffy, and L. W. Finger, Am. Mineral. **81**, 51 (1996).
- ⁴K. Takemura, K. Sato, H. Fujihisa, and M. Onoda, Ferroelectrics **305**, 103 (2004).
- ⁵C. S. Zha, T. S. Duffy, H. K. Mao, and R. J. Hemley, Phys. Rev. B **48**, 9246 (1993).
- ⁶C. S. Zha, T. S. Duffy, R. T. Downs, H. K. Mao, and R. J. Hemley, J. Geophys. Res. **101**, 17535 (1996).
- ⁷C. S. Zha, T. S. Duffy, H. K. Mao, R. T. Downs, R. J. Hemley, and D. J. Weindner, Earth Planet. Sci. Lett. **147**, E9 (1997).
- ⁸C. S. Zha, H. K. Mao, and R. J. Hemley, Phys. Rev. B **70**, 174107 (2004).
- ⁹J. P. Franck and R. Wanner, Phys. Rev. Lett. **25**, 345 (1970).
- ¹⁰R. Wanner and J. P. Franck, Phys. Rev. Lett. **24**, 365 (1970).
- ¹¹G. Ahlers, Phys. Rev. A **2**, 1505 (1970).
- ¹²R. L. Mills, D. H. Liebenberg, and J. C. Bronson, Phys. Rev. B **21**, 5137 (1980).
- ¹³A. Driessen, E. van der Poll, and I. F. Silvera, Phys. Rev. B **33**, 3269 (1986).
- ¹⁴H. K. Mao, R. J. Hemley, Y. Wu, A. P. Jephcoat, L. W. Finger, C. S. Zha, and W. A. Bassett, Phys. Rev. Lett. **60**, 2649 (1988).
- ¹⁵A. Dewaele, J. Eggert, P. Loubeyre, and R. Le Toullec, Phys. Rev. B **67**, 094112 (2003).
- ¹⁶D. A. Young, A. K. McMahan, and M. Ross, Phys. Rev. B **24**, 5119 (1981).
- ¹⁷P. Loubeyre, J. M. Besson, J. P. Pinceaux, and J. P. Hansen, Phys. Rev. Lett. **49**, 1172 (1982).
- ¹⁸P. Loubeyre, D. Levesque, and J. J. Weis, Phys. Rev. B **33**, 318 (1986).
- ¹⁹P. Loubeyre, Phys. Rev. Lett. **58**, 1857 (1987).
- ²⁰S.-Y. Chang and M. Boninsegni, J. Chem. Phys. **115**, 2629 (2001).
- ²¹T. Biben and D. Frenkel, J. Phys.: Condens. Matter **14**, 9077 (2002).
- ²²T. Tsuchiya and K. Kawamura, J. Chem. Phys. **117**, 5859 (2002).
- ²³P. Hohenberg and W. Kohn, Phys. Rev. **136B**, 864 (1964).
- ²⁴W. Kohn and L. J. Sham, Phys. Rev. **140A**, 1133 (1965).
- ²⁵O. K. Andersen, O. Jepsen, and G. Krier, in *Lectures on Methods of Electronic Structure Calculations*, edited by V. Kumar, O. K. Andersen, and A. Mookerjee (World Scientific, Singapore, 1994), p. 63.
- ²⁶L. Vitos, Phys. Rev. B **64**, 014107 (2001).
- ²⁷L. Vitos, I. A. Abrikosov, and B. Johansson, Phys. Rev. Lett. **87**, 156401 (2001).
- ²⁸L. Vitos, in *Recent Research Developments in Physics* (Transworld Research Network, Trivandrum, India, 2004), Vol. 5, pp. 103–140.
- ²⁹J. Kollár, L. Vitos, and H. L. Skriver, in *Electronic Structure and Physical Properties of Solids: The Uses of the LMTO Method*, Lectures Notes in Physics, edited by H. Dreyssé (Springer-Verlag, Berlin, 2000), p. 85.
- ³⁰J. P. Perdew and Y. Wang, Phys. Rev. B **45**, 13244 (1992).
- ³¹L. Vitos, B. Johansson, J. Kollár, and H. L. Skriver, Phys. Rev. B **62**, 10046 (2000).
- ³²J. P. Perdew, K. Burke, and M. Ernzerhof, Phys. Rev. Lett. **77**, 3865 (1996).
- ³³W. Kohn, Y. Meir, and D. E. Makarov, Phys. Rev. Lett. **80**, 4153 (1998).
- ³⁴P. Loubeyre, R. LeToullec, J. P. Pinceaux, H. K. Mao, J. Hu, and R. J. Hemley, Phys. Rev. Lett. **71**, 2272 (1993).
- ³⁵J. P. Franck and W. B. Daniels, Phys. Rev. Lett. **44**, 259 (1980).
- ³⁶C.-L. Fu and K.-M. Ho, Phys. Rev. B **28**, 5480 (1983).
- ³⁷G. Steinle-Neumann, L. Stixrude, and R. E. Cohen, Phys. Rev. B **60**, 791 (1999).
- ³⁸P. M. Marcus and S. L. Qiu, J. Phys.: Condens. Matter **16**, 8787 (2004).
- ³⁹G. Steinle-Neumann and R. E. Cohen, J. Phys.: Condens. Matter **16**, 8783 (2004).
- ⁴⁰D. A. Young, *Phase Diagrams of the Elements* (University of California, Berkeley, 1991).
- ⁴¹S. Kurth, P. J. Perdew, and P. Blaha, Int. J. Quantum Chem. **75**, 889 (1999).
- ⁴²P. Söderlind, O. Eriksson, J. M. Wills, and A. M. Boring, Phys. Rev. B **48**, 5844 (1993).
- ⁴³G. Grimvall, *Thermophysical Properties of Materials*, enlarged and revised edition (North-Holland, Amsterdam, 1999).
- ⁴⁴Landolt-Börnstein, in *Numerical Data and Functional Relationships in Science and Technology*, New Series, Group III (Springer-Verlag, Berlin, 1966), Vol. 1.
- ⁴⁵J. P. Watt and L. Peselnick, J. Appl. Phys. **51**, 1525 (1980).
- ⁴⁶D. H. Chung and W. R. Buessem, J. Appl. Phys. **38**, 2010 (1967).